4. Simulation of the Stress-Strain Behaviour of Coal Pillars

4.1 General

A realistic simulation of the stress-strain behaviour of the pillars is a primary requirement for the design of PWBP. The strain-softening parameters define the stress vs. strain behaviour of pillars. An extensive laboratory test done by Das (1986) incorporated the testing of coal samples with a w/h ratio of 0.5-13.5 for six Indian coal seams. This chapter describes the standard approach developed to simulate the laboratory-observed behaviour using the numerical modelling approach. A statistical model was developed based on the findings to decide the drop rate in cohesion, friction and dilation for a given zone size of elements in the numerical model. These findings formed the basis for studying the damage induced in the PWBP.

4.2 Laboratory Test

Laboratory tests were conducted on cylindrical coal samples of 54 mm diameter for the w/h ratio of 0.5–10 to obtain their post-failure behaviour. The test samples were prepared in the workshop of the Rock Mechanics Laboratory of the Department of Mining Engineering of IIT (BHU), Varanasi. The samples were cut for the desired w/h ratio and polished at the edges for smoothening of the end surfaces. The tests were conducted on the Stiff Material Testing System (MTS) installed at the laboratory (Figure 4.1). A constant loading was applied at the rate of 0.005 mm/step. The stress-strain curves (Figure 4.2) were obtained as output from the MTS. The behaviour transitions from brittle to strain-softening to strain-hardening as the w/h ratio increases from 0.5 to 10. The test results confirmed the previous findings reported by Das (1986). The visual observation in samples having a w/h ratio of 10 confirmed formations

of three distinct zones, as shown in Figure 4.3 (Morsy, 2003; Prassetyo, 2011). The innermost zone remained intact, while the middle zone II yielded but did not crush. The outermost zone III formed the crushed and slumped portion of the specimens.

Figure 4.1. Material Testing System (MTS) facility used for coal testing at IIT (BHU), Varanasi

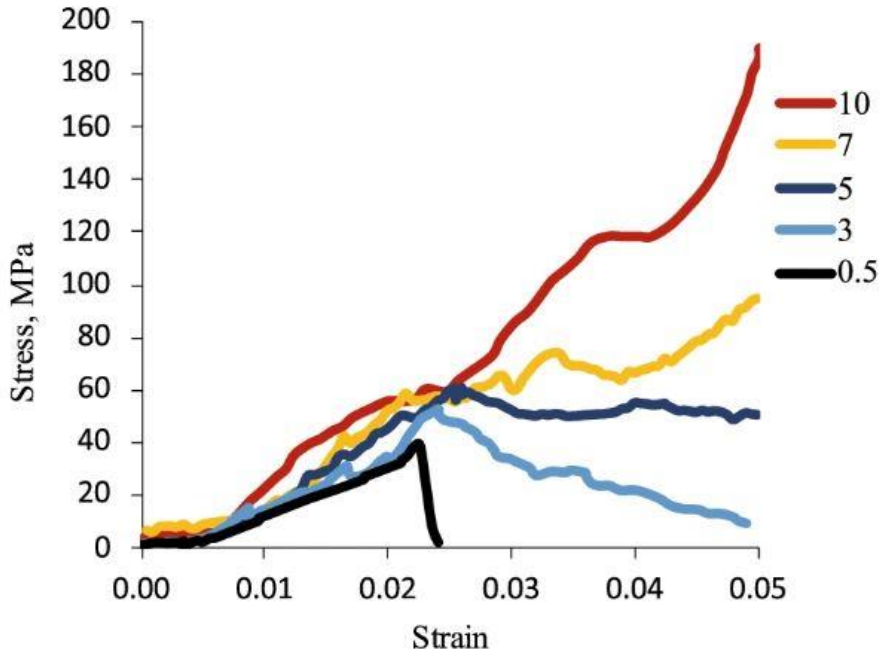

Figure 4.2. Laboratory observed stress-strain behaviour of coal samples for a w/h ratio of 0.5 -10

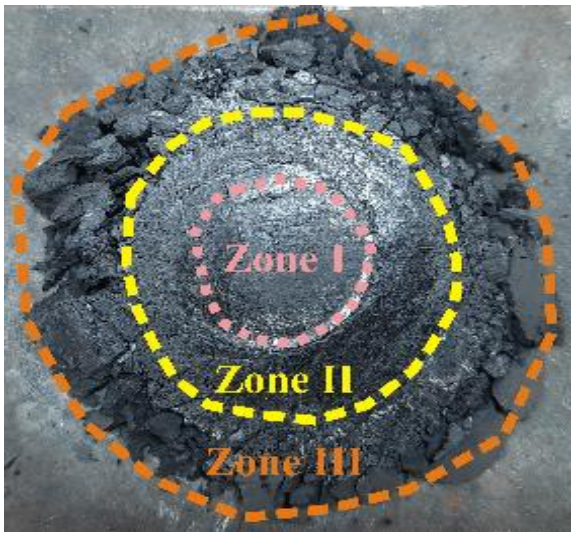

Zone I: Intact Zone

Zone II: Yielding Zone

Zone III: Crushed + Slumped Zone

Figure 4.3. zones identified on the top end surface of a coal sample of w/h=10

4.3 Numerical Simulation of Laboratory Observed Behaviour

Axisymmetric models were run in FLAC 2D to simulate the constitutive behaviour of the coal specimen. The model incorporated the specimen of a given w/h ratio along with the loading platens at the top and bottom. The platens were designed as per the ISRM standard wherein the diameter of the platen should be between D and D+2, and its thickness should be at least 15 mm, or one-third of the specimen diameter (D) (Fairhurst and Hudson 1999). For a coal specimen of 54 mm diameter, the platen's diameter was 56 mm, while its thickness was 18 mm. The height of the specimen was varied to obtain a w/h ratio varying from 0.5-13.5. The modelled specimen was placed in the centre of the platens to facilitate uniform loading.

The model was discretized uniformly with the desired element size. The lower and upper platens were bonded with the specimen through an interface in-between to allow slippage and simulate realistic confinement. The constitutive behaviour of the coal specimen was found to be critically dependent upon the interface properties (Peng, 1978; Wagner, 1980; Iannacchione, 1990; Prassetyo, 2011; Rashed and Peng, 2015; Lonnies, 2017). A detailed discussion of related observations is given in Chapter 2 and Chapter 3, Section 3.2.3. The interface properties given in Table 4.1 were used for simulation.

Displacement-constrained conditions were initialised at the top and bottom platens of the model, and their x and y displacements were fixed. A constant compressive velocity of 10^{-5} mm/timestep was applied at the top and bottom of the model. The histories of a few monitoring parameters were set before solving the model for the desired number of steps up to monitor the load-deformation characteristic of the specimen up to their residual strength. Further analysis of the model output was done in terms of induced vertical and horizontal

stresses, axial and lateral strain, dilation angle, volumetric strain, and differential stress with the help of the recorded history log files.

Table 4.1. Interface properties used in the models

Property	Value	Comment
Normal and shear Stiffness, GPa/m	$10\frac{\left(B+\frac{4}{3}G\right)}{\Delta z_{min}}$	Δz_{min} is the minimum zone size along the interface, bulk, B, and shear moduli, G should be of the softer material along the interface (ITASCA 2011)
Cohesion, MPa	0	
Tensile strength, MPa	0	Lonnies (2017)
Friction angle, °	14	Rashed and Peng (2015)
Dilation angle, °	5	

4.4 Parametric Study

The post-failure behaviour, such as post-peak and residual strength, and the post-failure modulus of the coal material depend on the strain-softening parameters and the size of discretised elements. Hence, the model parameters were calibrated to establish validated relationships for estimating the drop rate, residual cohesion, and friction angle values to replicate the laboratory-observed behaviour. A parametric study was done to simulate the observed laboratory behaviour for six Indian coal seams for various w/h ratio specimens (Table 4.2).

Table 4.2. Coal properties for Indian coal seams (Das, 1986; Das and Sheorey, 1986; Sheorey et al., 1986)

Seam	Elastic Modulus, GPa	Shear Modulus, GPa	Bulk Modulus, GPa	UCS, MPa	Tensile strength, MPa	Cohesion, MPa	Friction angle, °
Kenda	2.70	1.08	1.80	47.48	3.17	10.34	43
Jambad	2.40	0.96	1.60	40.30	2.69	7.15	51
Kargali	4.00	1.60	2.67	31.00	2.07	8.08	35
Singhpur	4.87	1.95	3.25	37.40	2.49	7.95	44
Uchitdih	1.82	0.73	1.21	20.00	1.33	4.15	45
XII	2.46	0.98	1.64	19.50	1.30	3.95	46

This study considered a linearized softening law for cohesion, friction angle and dilation angle mobilisation as a function of plastic shear strain (Figures 4.4,4.5). The linearised cohesion reduction was implemented with plastic shear strain in the Mohr-Coulomb strain softening model. The peak value of the friction angle was reduced at a specific drop rate up to its residual value. The peak values of cohesion (C_{peak}), and friction angle (ϕ_{peak}) represented the rock mass cohesion and friction angle, respectively. The residual cohesion (CR) and friction angle (FR) were calculated as percentages of the C_{peak} and ϕ_{peak}, respectively. The cohesive strength and friction angle was reduced to residual cohesion ($\boldsymbol{c_{res}}$) and friction angle (ϕ_{res}) following a constant negative drop rate, defined by the slope of the straight lines connecting C_{peak} and c_{res}, and ϕ_{peak} and ϕ_{res} over a plastic shear strain ($\in_{ps}$), respectively. The drop rates were used to calculate the $\in_{ps}$, corresponding to the residual values of cohesion and friction angle. The values of (C_{peak}, C_{res}, CD, $\in_{ps}^{C}$), and (ϕ_{peak}, ϕ_{res}, FD, $\in_{ps}^{\phi}$) were used to generate strain-softening tables of 15 entries between their peak and residual limits.

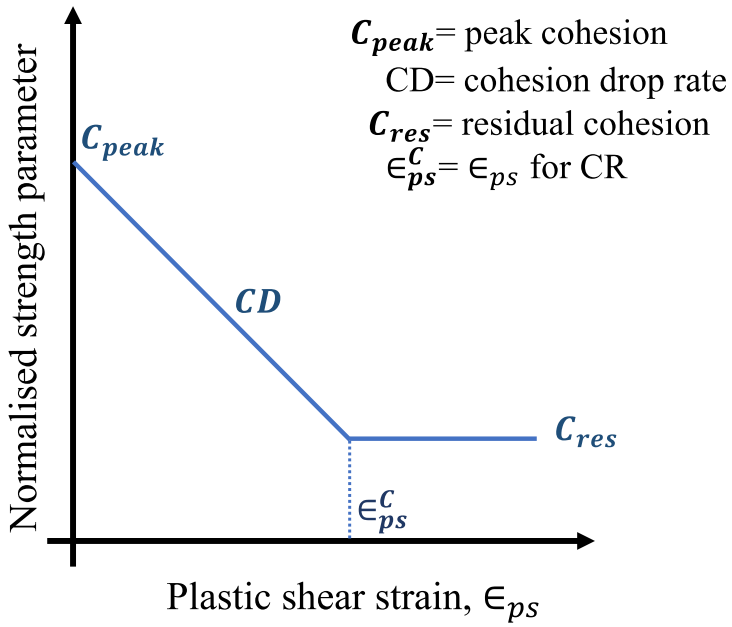

Figure 4.4. Schematic sketch of cohesion variation with plastic shear strain

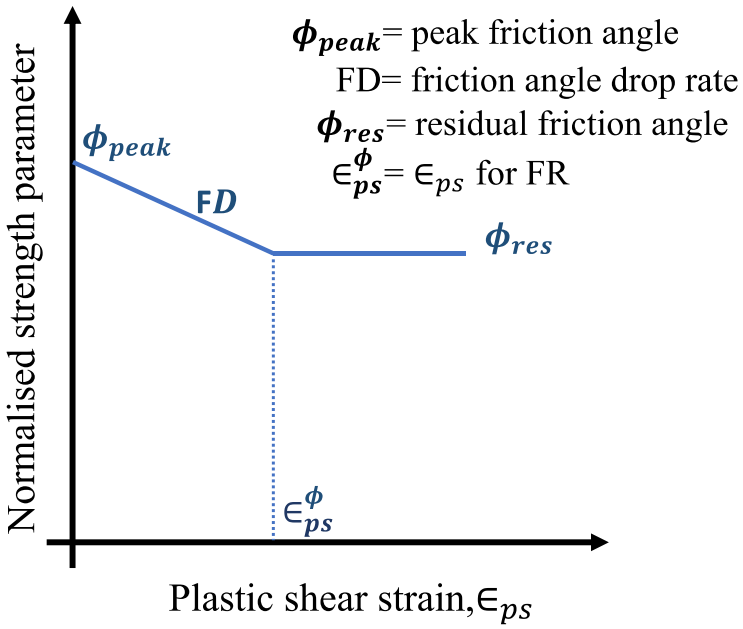

Figure 4.5. Schematic sketch of friction angle variation with plastic shear strain

The parametric study considered a w/h ratio of 0.5–13.5, zone size varying from 0.5 mm × 0.5 mm to 2 mm × 2 mm, cohesion drop (CD) rate up to 250 MPa/plastic shear strain, residual cohesion (CR) up to 100% of peak cohesion, friction angle reduction (FR) rate ranging from 100–500 °/plastic shear strain, and residual friction (FR) up to 90% of peak friction angle. The variation in dilation angle considered the Walton and Diederich model (2015), as discussed in Section 2.5, Chapter 2. A FISH module was developed for its implementation. The values of the associated input parameter used in the numerical model included α_0 = 0.17, α' = 0.045, γ_m = 0.001, γ_0 = 0.12, and γ^* = 0.025, as suggested by Walton and Diederichs (2015).

The methodology shown in Figure 4.6 was used to estimate the best-fit strain-softening parameters for a particular condition. If the desired stress-strain behaviour is not observed for the set of initial values, the next set of drop rates and residual values were assigned in the model. If the model peak strength observed was lesser than the laboratory observed values, the CD and FD were decreased, and vice versa. However, the CR and FR were increased if the model-observed residual strength was smaller than the laboratory-observed strength and vice versa. This approach helped in obtaining the desired results and matching the model-observed behaviour with the laboratory observations without lot of experimental iterations.

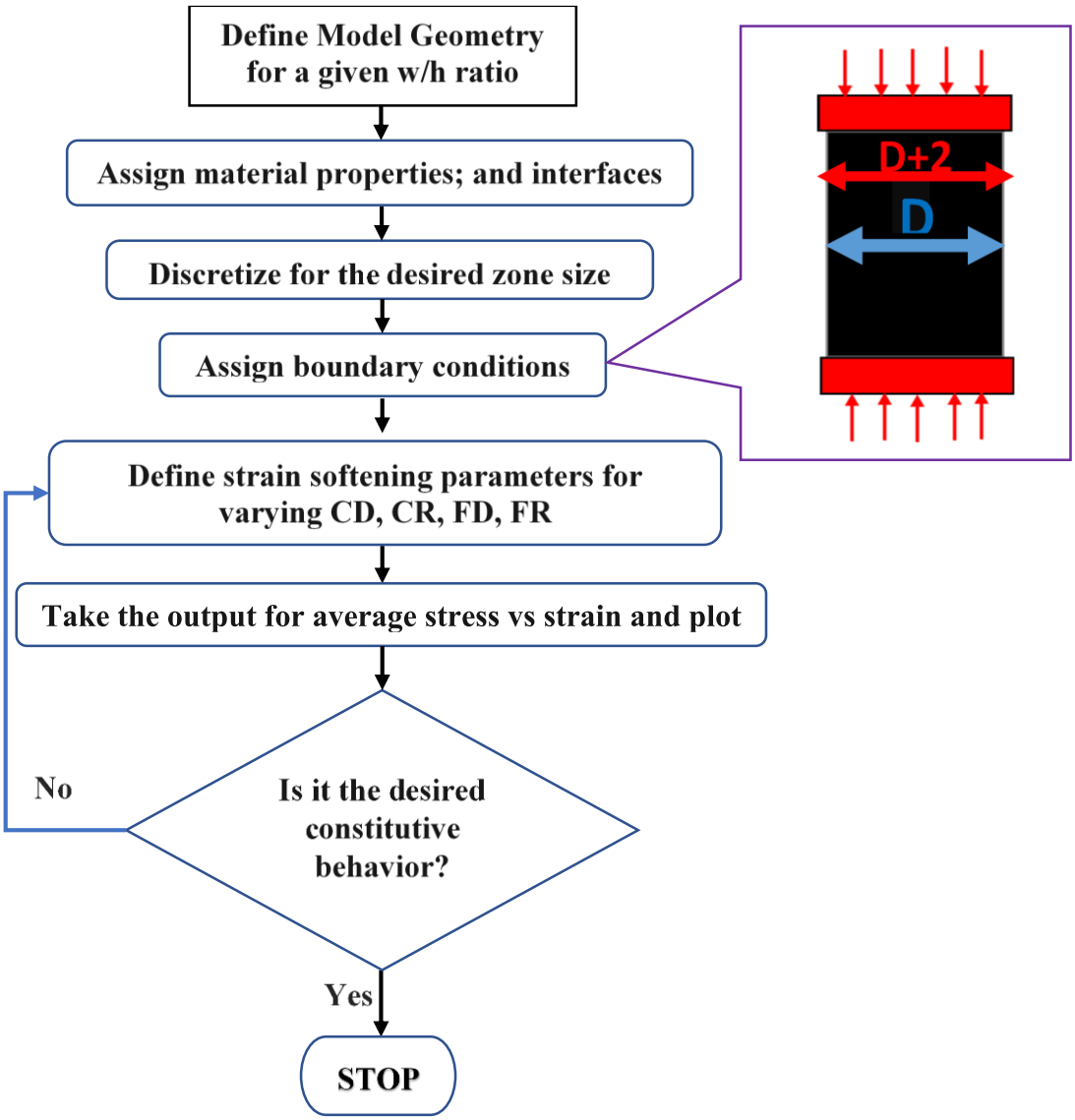

Figure 4.6. Methodology for estimating the best-fit strain softening rule

Thousands of models were run to obtain the best match of the laboratory findings reported by Das (1986) using a trial-and-error approach. Firstly, the models were run by varying the cohesion drop rate and their residual values only. At the subsequent stage, the friction angle drop rate and their residual values were varied for different combinations of the CD, CR, FD, and FR to match the stress vs. strain behaviour of the modelled specimen with their laboratory-observed behaviour.

Figure 4.7 shows the comparative plot of the best-fit stress-strain characteristics obtained from the model and the laboratory-observed behaviour for the Kenda coal seam. The peak strength, residual strength, and trend of the stress-strain curve matched well with the laboratory findings. As the w/h ratio increased from 0.5 to 13.5, the stress-strain behaviour migrated from brittle to strain softening to perfectly plastic to strain hardening. The model outcomes were matched for the other five seams in a similar manner for a w/h ratio varying from 0.5 to 13.5 and a zone size of 0.5-2 mm.

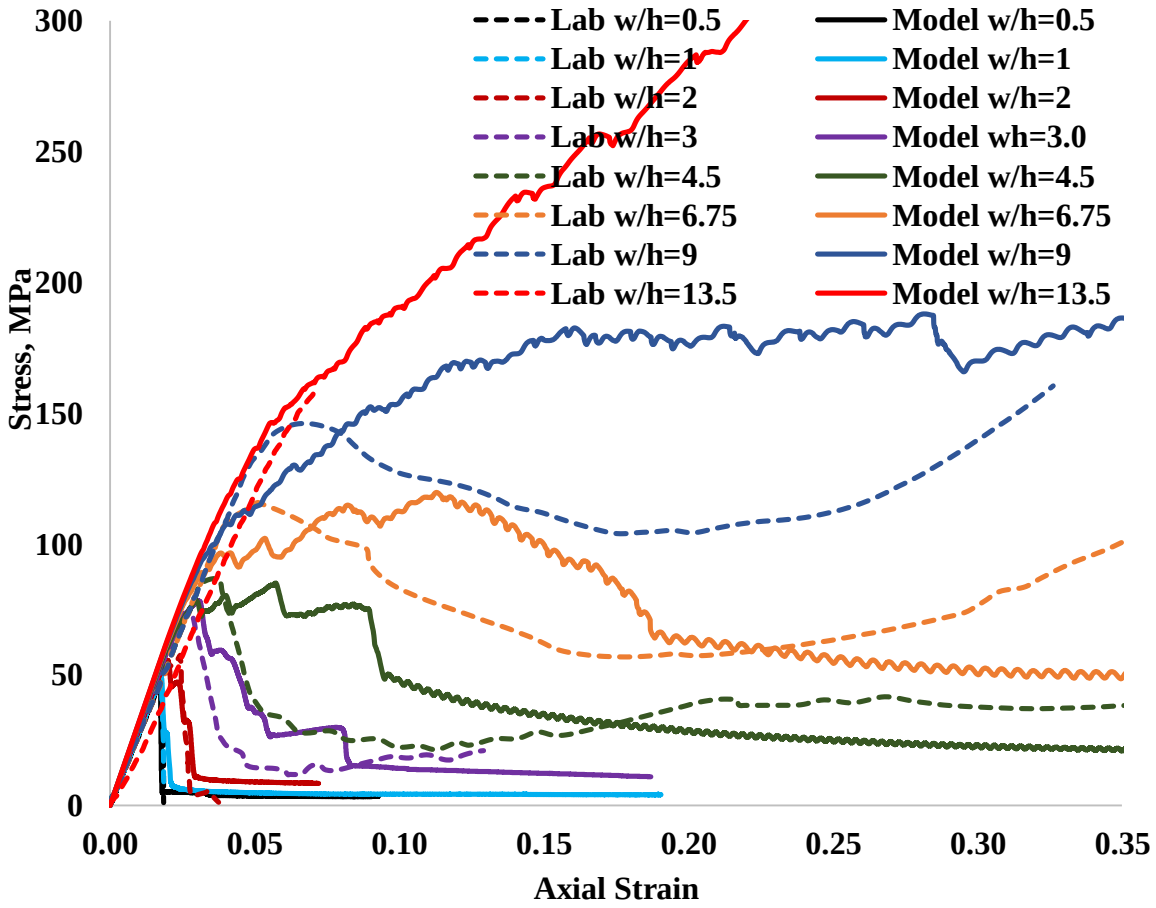

Figure 4.7. A comparative plot of the model and laboratory observed stress-strain behaviour of Kenda Seam coal specimens having a w/h ratio of 0.5-13.5 and zone size of 0.5 mm

Figure 4.8 shows the plot of the volumetric vs. axial strain corresponding to the best fit stress-strain plots of the Kenda seam coal specimens. The stress-strain behaviour for the specimens corresponded well with the expected trends of axial vs. volumetric strain, explaining the dilatancy of the material. The formation of large-size cracks observed during laboratory tests of specimens having smaller w/h was characterised by brittle post-failure behaviour and reversal of strain on the axial vs. volumetric strain plots in the numerical models in the absence of confinement. However, the confinement increased for higher w/h ratio specimens, creating compaction over disintegration, as evidenced by an increase in positive volumetric strain with the axial strain.

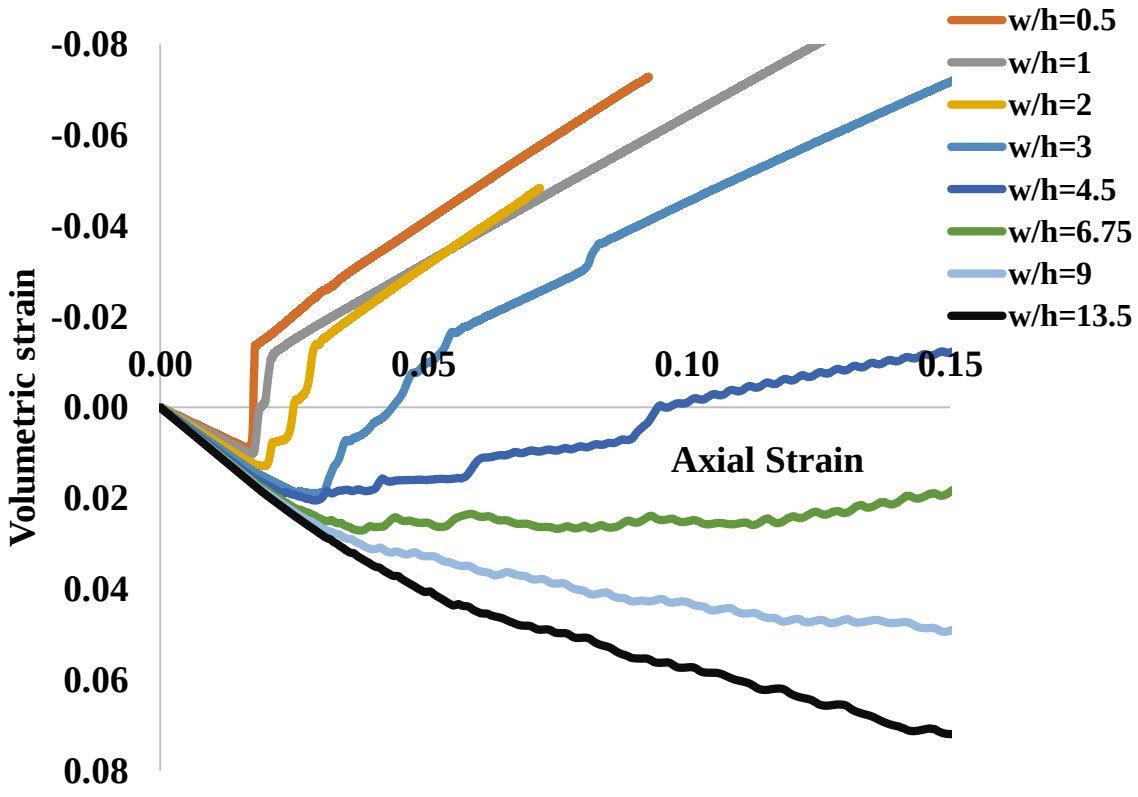

Figure 4.8. Volumetric strain vs axial strain for w/h ratio 0.5-13.5 and zone size of 0.5 mm for Kenda Seam (Positive sign indicates compression)

4.5 Statistical Model for Strain-Softening Parameters

Table 4.3 summarises the best-fit results of CD, CR, FD, and FR for zone sizes of 0.5, 1, and 2 mm for coal specimens having w/h ratios of 0.5, 1.0, 2.0, 3.0, 4.5, 6.75, 9.0, and 13.5 for the six Indian coal seams. The increase in drop rates of cohesion and friction reduced the peak strength, and the increase in residual cohesion and friction angle increased the residual strength. The model outcome was influenced by the drop rates in cohesion and friction angle and their residual values, but it was more sensitive to the cohesion drop rate and its residual value. The zone size significantly influenced the stress-strain behaviour of the specimens. The peak and residual strength of the samples increased with the zone size.

Table 4.3. Best fit cases of CD, CR, FD, and FR for strain-softening behaviour of coal

Seam	w/h	Zone_size	CD	CR	FD	FR
Jambad Top	0.5	2	100	0	100	50
Jambad Top	0.5	1	60	0	100	50
Jambad Top	0.5	0.5	18	0	100	50
Jambad Top	2	2	100	0	100	50
Jambad Top	2	1	60	0	100	50
Jambad Top	2	0.5	18	0	100	50
Jambad Top	3	2	100	5	300	50
Jambad Top	3	1	80	5	300	50
Jambad Top	3	0.5	22	5	300	50
Jambad Top	4.5	2	70	10	300	50
Jambad Top	4.5	1	50	10	300	50
Jambad Top	4.5	0.5	20	10	300	50
Jambad Top	6.75	2	50	15	500	50
Jambad Top	6.75	1	40	15	500	50
Jambad Top	6.75	0.5	25	15	500	50
Jambad Top	9	2	50	20	500	50
Jambad Top	9	1	40	20	500	50
Jambad Top	9	0.5	30	20	500	50
Jambad Top	13.5	2	50	20	500	50
Jambad Top	13.5	1	40	20	500	50
Jambad Top	13.5	0.5	30	20	500	50

Kargali	0.5	2	180	0	100	50
Kargali	0.5	1	110	0	100	50
Kargali	0.5	0.5	35	0	100	50
Kargali	2	2	180	0	100	50
Kargali	2	1	110	0	100	50
Kargali	2	0.5	35	0	100	50
Kargali	3	2	160	5	300	50
Kargali	3	1	140	5	300	50
Kargali	3	0.5	45	5	300	50
Kargali	4.5	2	210	10	300	50
Kargali	4.5	1	190	10	300	50
Kargali	4.5	0.5	60	10	300	50
Kargali	6.75	2	130	15	300	70
Kargali	6.75	1	150	15	300	70
Kargali	6.75	0.5	65	15	300	70
Kargali	9	2	90	20	500	70
Kargali	9	1	120	20	500	70
Kargali	9	0.5	65	20	500	50
Kargali	13.5	2	90	20	500	70
Kargali	13.5	1	120	20	500	70
Kargali	13.5	0.5	65	20	500	50
Kenda	0.5	2	220	0	100	50
Kenda	0.5	1	140	0	100	50
Kenda	0.5	0.5	30	0	100	50
Kenda	2	2	160	0	100	50
Kenda	2	1	130	0	100	50
Kenda	2	0.5	40	0	100	50
Kenda	3	2	140	5	300	50
Kenda	3	1	90	5	300	50
Kenda	3	0.5	50	5	300	50
Kenda	4.5	2	100	10	500	70
Kenda	4.5	1	70	10	300	50
Kenda	4.5	0.5	60	10	500	50
Kenda	6.75	2	90	15	500	50
Kenda	6.75	1	70	15	500	50
Kenda	6.75	0.5	60	15	500	50
Kenda	9	2	90	20	500	50
Kenda	9	1	70	20	500	50
Kenda	9	0.5	60	20	500	50
Kenda	13.5	2	220	20	500	50
Kenda	13.5	1	140	20	500	50
Kenda	13.5	0.5	30	20	500	50
Singhpur Middle	0.5	2	230	0	100	50
Singhpur Middle	0.5	1	160	0	100	50

Singhpur Middle	0.5	0.5	30	0	100	50
Singhpur Middle	2	2	230	0	100	50
Singhpur Middle	2	1	160	0	100	50
Singhpur Middle	2	0.5	30	0	100	50
Singhpur Middle	3.2	2	250	5	500	70
Singhpur Middle	3.2	1	210	5	300	50
Singhpur Middle	3.2	0.5	100	5	500	50
Singhpur Middle	4.5	2	200	10	500	70
Singhpur Middle	4.5	1	190	10	300	50
Singhpur Middle	4.5	0.5	130	10	500	50
Singhpur Middle	7.7	2	190	15	500	70
Singhpur Middle	7.7	1	190	15	500	50
Singhpur Middle	7.7	0.5	150	15	500	50
Singhpur Middle	9	2	180	20	500	50
Singhpur Middle	9	1	180	20	500	50
Singhpur Middle	9	0.5	170	20	500	50
Singhpur Middle	13.5	2	180	20	500	50
Singhpur Middle	13.5	1	180	20	500	50
Singhpur Middle	13.5	0.5	170	20	500	50
Uchitdih	0.5	2	60	0	100	50
Uchitdih	0.5	1	25	0	100	50
Uchitdih	0.5	0.5	8	0	100	50
Uchitdih	2	2	60	0	100	50
Uchitdih	2	1	25	0	100	50
Uchitdih	2	0.5	8	0	100	50
Uchitdih	3	2	50	5	500	50
Uchitdih	3	1	25	5	500	50
Uchitdih	3	0.5	10	5	500	50
Uchitdih	4.5	2	40	10	300	50
Uchitdih	4.5	1	50	10	500	50
Uchitdih	4.5	0.5	20	10	500	50
Uchitdih	6.75	2	40	15	300	50
Uchitdih	6.75	1	50	15	500	50
Uchitdih	6.75	0.5	30	15	500	50
Uchitdih	9	2	20	20	500	50
Uchitdih	9	1	25	20	500	50
Uchitdih	9	0.5	20	20	500	50
Uchitdih	13.5	2	20	20	500	50
Uchitdih	13.5	1	25	20	500	50
Uchitdih	13.5	0.5	20	20	500	50
XII	0.5	2	70	0	100	50
XII	0.5	1	40	0	100	50
XII	0.5	0.5	20	0	100	50
XII	2	2	70	0	100	50

XII	2	1	40	0	100	50
XII	2	0.5	20	0	100	50
XII	3	2	70	5	500	50
XII	3	1	50	5	300	50
XII	3	0.5	20	5	300	50
XII	4.5	2	40	10	500	70
XII	4.5	1	40	10	300	70
XII	4.5	0.5	20	10	300	50
XII	6.75	2	40	15	500	70
XII	6.75	1	60	15	500	70
XII	6.75	0.5	30	15	300	50
XII	9	2	30	20	500	70
XII	9	1	30	20	500	50
XII	9	0.5	20	20	500	50
XII	13.5	2	30	20	500	70
XII	13.5	1	30	20	500	50
XII	13.5	0.5	20	20	500	50

The best-fit findings were subsequently used to establish the statistical models (Equations 4.1–4.4) for estimating cohesion and friction drop and their residual values as a function of the compressive strength, friction angle, elastic modulus, w/h ratio, and zone size.

$$CD = \frac{22.49\sigma_c^{0.63}E^{1.42}Z_S^{0.60}}{\left(\frac{w}{h}\right)^{0.06}\phi_{peak}^{0.65}}, \qquad R^2 = 0.76 \qquad \ldots(4.1)$$

$$CR = \begin{cases} 0 & \forall\ w/h \leq 2 \\ 11.43\ln\left(\frac{w}{h}\right) - 7.33 & \forall\ w/h > 2, \quad R^2 = 0.96 \end{cases} \qquad \ldots(4.2)$$

$$FD = \begin{cases} 100 & \forall\ w/h \leq 2 \\ 300\ or\ 500 & \forall\ 2 < w/h < 6.75 \\ 500 & \forall\ w/h \geq 6.75 \end{cases} \qquad \ldots(4.3)$$

$$FR = 50 \qquad \ldots(4.4)$$

Where, CD = rate of cohesion drop, MPa/plastic shear strain,

FD = rate of friction drop, °/plastic shear strain,

CR = residual cohesion, % of peak cohesion,

FR = friction residual, % peak friction angle,

σ_c = the compressive strength, MPa,

E = modulus of elasticity, GPa,

Z_s = zone size, m,

w = width of the specimen, m,

h = height of the specimen, m, and

ϕ_{peak} = peak friction angle, °.

4.6 Summary

A numerical modelling study was carried out to reproduce the laboratory-observed stress-strain behaviour for coal specimens of different w/h ratios and understand the sensitivity of various imperative parameters to this effect. The Mohr-Coulomb strain-softening parameters, such as peak cohesion and frictional angle, and their residual values and corresponding plastic shear strain were transformed into CD, FD, CR, and FR. A set of statistical relations were established for determining these parameters using best-fit outcomes obtained after extensive trial-and-error experimentation for element size of 0.5–2.0 mm and w/h ratios of 0.5–13.5 for six different Indian coal seams. The UCS of these coal specimens varied from

19.5-47.5 MPa, while their Young's modulus varied from 1.82-4.0 GPa, and their peak cohesion and friction angle varied from 3.95-10.34 MPa and 35-51°, respectively.

The calibrated numerical models provided an opportunity to investigate the failure mechanism for different w/h ratios of pillars. The study showed that the pillars of a w/h ratio less than 4.5 produced higher volumetric expansion as compared to their compaction resulting in a reversal of strain in the absence of significant confinement during the process of loading. However, larger pillars did not exhibit such reversal, and they continued to produce a positive volumetric strain with the progress of axial strain beyond the strain corresponding to the peak strength. This implied that pillars of lower w/h ratio could undergo sudden failure under loading exceeding their ultimate strength. However, pillars having a larger w/h ratio would experience only a progressive failure.